Staged Z pinch for controlled fusion

P. Ney and H. U. Rahman
Institute of Geophysics and Planetary Physics, University of California, Riverside, California 92521

F. J. Wessel and N. Rostoker
Department of Physics, University of California, Irvine, California 92717

(Received 11 January 2000; accepted 8 November 2000)

A staged Z pinch is considered in which an annular plasma shell made of a high Z material like Kr implodes onto a coaxial plasma target made of a low Z material like deuterium or a deuterium–tritium mixture. The target plasma could be made either by exploding a cryogenically extruded fiber or by filling the annular shell with a gas puff or a plasma puff. Modeling is performed with a two-dimensional (2D) radiation-MHD (magnetohydrodynamic) code. A parameter study is made to determine the sensitivity of this configuration to initial conditions of the shell and the target plasmas. An axial magnetic field is essential for a stable implosion and efficient energy coupling to the final load. Using a 50–50 mixture of deuterium–tritium as a target plasma, the fusion energy gain is optimized by adjusting the initial parameters. The calculations are based on the parameters of the University of California Irvine Z-pinch facility which has a maximum energy storage of 50 kJ.
 [DOI: 10.1063/1.1339230]

I. INTRODUCTION

The conventional Z pinch consists of a simple cylindrical load which implodes due to a self generated azimuthal magnetic field produced by an axial current through the load. The current profile is usually in a pulsed form with a characteristic rise time determined by the circuit parameters. Although the Z pinch provides a mechanism for the direct conversion of electrical energy into thermal energy of the plasma, energy coupling is not very effective. This is primarily due to radiation losses and the unstable nature of the imploding plasma column. Both these effects become worse in machines which have relatively slow rising current profiles. A new class of machine with an extremely fast current rise time ($dI/dt \approx 10^{14}$ A/s), e.g., PBFAZ,[1] Saturn,[2] etc., has been developed to overcome some of these problems. Recent results have shown remarkable improvement, both in energy coupling and the stability of the imploding Z-pinch plasma column. In particular, on a 20 MA Z facility at Sandia National Laboratories, tungsten wire array implosions have generated x-ray powers of up to 280 TW[3] with a total radiated energy of 1.75 MJ, which was ≈58% of the total input electrical energy. Modeling performed by the same code used in the present study has attributed this enhanced level of energy coupling to a lower level of growth of Rayleigh–Taylor instability.

Z pinches are inherently unstable mainly due to Rayleigh–Taylor (RT) instability which appears during the run-in phase of the pinch. The reason for the growth of this instability is the development of a steep density gradient across an accelerating interface between the plasma and the magnetic field. There are several ways to control or at least mitigate some of the most dangerous modes associated with RT-type instabilities.[4–12] Some of these methods have been successfully implemented on several facilities. Even if by some mechanism the RT-instability is controlled, the plasma column becomes unstable in its final phase of implosion during stagnation, because of the rapid growth of magnetohydrodynamic (MHD) instabilities. These instabilities are usually unavoidable in conventional Z pinches and have been observed in almost every Z pinch experiment. The most dangerous modes of MHD instabilities are the sausage ($m=0$) mode and the kink ($m=1$) mode that can virtually destroy the uniformity of the cylindrical plasma column. The upper limit on the growth time of these instabilities is the Alfvén time scale $\tau_A \approx a/v_A$, where a is the radius of the plasma column and v_A is the Alfvén velocity. Unless the stagnation time of the pinch is faster than the Alfvén time scale, these instabilities will certainly appear and disrupt the pinch. Trapping an axial magnetic field inside the plasma column will develop an outward magnetic pressure which will hinder the growth of the sausage instability. On the other hand, an azimuthal magnetic field outside the pinch with a trapped axial magnetic field inside the pinch can lead to a sheared magnetic field profile that can easily stop the growth of the RT-instability provided it is maintained during the implosion. As a disadvantage, the trapping of a magnetic field inside the plasma column leads to a softer pinch. However, the axial magnetic field alone does not stabilize the kink or higher m modes, but these modes usually have a much higher growth time as compared to the stagnation time of a staged Z pinch. The chances of developing these modes in a fast pinch are very low.

The staged Z pinch in general[13,14] corresponds to a wide range of configurations, e.g., Z–Z pinch, Z–θ pinch,[15] composite pinch,[16] nested wire array,[3] puff on puff, etc. All these configurations usually involve similar types of physical mechanisms for coupling energy from one load to another. Experiments have shown that these pinches are relatively stable and provide much better coupling of energy to the final load. In this paper we focus on one of the simplest of

the staged Z-pinch configurations which is basically the combination of a Z–Z pinch and a Z–θ pinch. This scheme stabilizes most of the dangerous instabilities associated with the conventional Z pinch. As a result higher compression leading to a much higher energy density Z pinch can be achieved. In this scheme the load plasma is made from two coaxial cylindrical plasma columns. The outer plasma column is a cylindrical shell made of Kr plasma which is highly radiative, and thus remains cold during the implosion. Since the resistivity of the plasma goes as $T^{-3/2}$, the magnetic field can easily diffuse through such a resistive plasma shell. The inner plasma column on the other hand is made of a deuterium or a deuterium–tritium (DT) mixture which does not radiate heavily as it heats up. An axial magnetic field is applied externally throughout the entire region of the load plasma. During the implosion, the combination of axial and azimuthal magnetic field components create a sheared magnetic field profile that maintains the stability of the outer shell as the implosion progresses. On the other hand the target plasma is less radiative and therefore continuously heats up during the implosion. The magnetic field cannot easily diffuse through this plasma. As a result it leads to an interesting configuration, in which most of the magnetic flux is trapped in between the inner and outer plasmas. As the implosion proceeds the intensity of the trapped magnetic field rises due to the compression of magnetic flux. This will sustain the required amount of shear in the magnetic field profile which is necessary for the stability of the pinching plasma shell. On the other hand the inner pinch will either remain flux free or will retain a highly reduced level of magnetic field. In the final phase of pinch the energy density of the target plasma achieves a remarkably large value due to the stable implosion and remains almost perfectly uniform up until the peak implosion. After peak implosion when the plasma column bounces back due to an increased level of the internal pressure, the MHD instabilities start growing rapidly.

In this paper we present a numerical study based on a two-dimensional MHD-modeling of this type of staged pinch and demonstrate the stable implosion that results in achieving a high energy density target plasma. Intense generation of soft x-rays and/or neutrons may be achieved by properly choosing the load parameters and applying the appropriate strength of B_z. Our main purpose in this study is to investigate the possibility of achieving high yield controlled thermonuclear fusion energy using a low energy ($\approx$50 kJ) electrical driver. The incentive for choosing a low energy driver is its high repetition rate. Multi-megajoule class machines are normally operated in a single shot mode and after each shot the entire load region has to be replaced. In this paper, in Sec. II we describe the description of the code and the simulation model. In Sec. III we describe the results of the simulation for a staged Z pinch using the University of California at Irvine (UCI) machine parameters showing the optimum initial conditions and the effect of axial magnetic field on the stability of the pinch. In Sec. IV we provide the conclusion of this paper.

II. SIMULATION MODEL

The staged Z pinch is a complex configuration and it is hard to simulate all features of the multi-shell imploding plasmas. To begin with, it consists of a circuit capable of producing a pulsed current of extremely high magnitude which requires a sophisticated circuit equation to model it accurately. The circuit equation can only provide a current profile with respect to time. The current has to flow through a coaxial load of two completely different types of plasmas. The outer shell of the load is made of a highly radiative plasma like Kr carrying almost the entire mass of the load. The inner coaxial column is made of a hydrogenic plasma with an insignificant mass as compared to the Kr shell. Both these plasmas can be modeled by magnetohydrodynamic (MHD) type equations but the true simulation of the outer plasma requires a radiation model that can correctly evaluate physical properties like resistivity, diffusivity, etc. The current produced by the generator flows through the combination of load plasmas in a complex spatial profile following path of the lowest impedance which shifts rapidly during the implosion and stagnation. Initially the lowest inductive path is the outer surface of the Kr plasma shell but the lowest resistive path is the inner core of the hydrogenic plasma that becomes hot during the implosion. Thus the preferential path of current flow initially is through the outer surface, but towards peak implosion the current switches to the inner load because of its highly conductive nature and almost similar value of inductance. Since the combination of an axial magnetic field B_z with an azimuthal magnetic field B_θ is very important for the stability and energy coupling of the staged Z pinch, the model must be capable of treating all three components of the magnetic field. Keeping all these factors in mind, the MACH2[17,18] code developed by the Phillips laboratory seems to be the most appropriate for modeling of the staged Z pinch.

MACH2 is a single fluid, two-and-a-half-dimensional ($2\frac{1}{2}$D), time dependent MHD code. It calculates resistive and thermal diffusion using various models for transport coefficients. It treats electron, ion and radiation temperatures separately. The equation of state can be calculated using analytical or tabular (SESAME) models. The code has the capability of calculating flux limited, single group, implicit radiation diffusion. The treatment of the generalized Ohm's law includes explicit Hall effect and thermal source terms for magnetic fields. This code can handle complex experimental shapes with a cylindrical or planar symmetry. It can handle multiple materials and has the capability of including material strength. The computation can be carried out either in Lagrangian, Eulerian or mixed mode.

The fusion neutron production rate and energy gain are calculated using

$$P_{\mathrm{DT}} = 5.6\times 10^{-13} n_{\mathrm{D}} n_{\mathrm{T}} (\overline{\sigma\nu})_{\mathrm{DT}},$$

$$P_{\mathrm{DD}} = 3.3\times 10^{-13} n_{\mathrm{D}} n_{\mathrm{D}} (\overline{\sigma\nu})_{\mathrm{DD}},$$

where $(\overline{\sigma\nu})_{\mathrm{DT}}$ and $(\overline{\sigma\nu})_{\mathrm{DD}}$ are determined from a table look up.

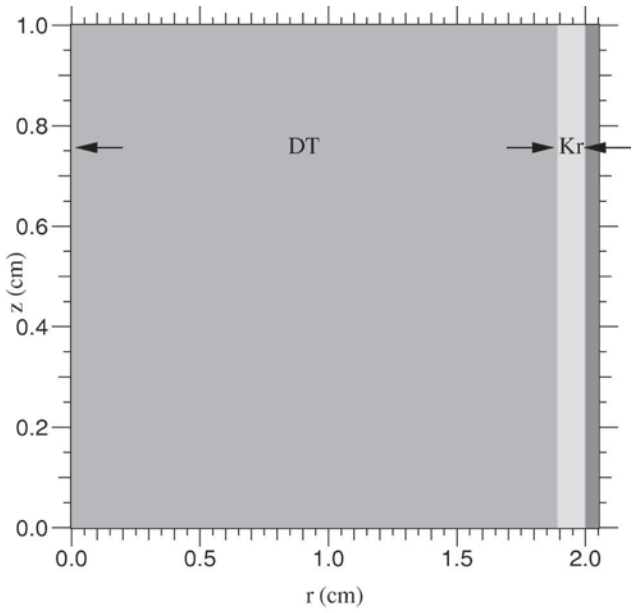

FIG. 1. Initial density profile of a 4 cm diameter Kr gas puff shell filled with DT.

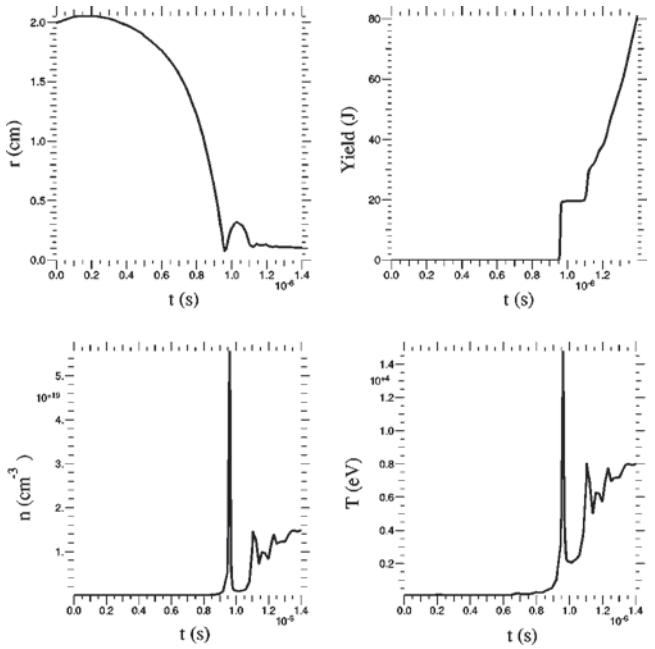

FIG. 3. Plots of pinch radius $r(t)$, axial plasma density $n(t)$, axial plasma temperature $T(t)$, and fusion yield $Y(t)$ versus time obtained from a 1-D simulation run for $B_z = 2$ KG.

The model solves the following set of MHD equations:
Continuity equation:

$$\frac{\partial \rho}{\partial t} = -\nabla \cdot (\rho \mathbf{v});$$

momentum equation:

$$\rho \frac{\partial v^i}{\partial t} = -\rho v^j \nabla_j v^i + \nabla_j \left[-(P+Q) g^{ji} + \sigma^d_{ji} + \frac{1}{\mu_0} \left(B^j B^i - \frac{1}{2} B^2 g^{ji} \right) \right];$$

electron specific energy equation:

$$\rho \frac{\partial \epsilon_e}{\partial t} = -\rho \mathbf{v} \cdot \nabla \epsilon_e - P_e g^{ji} \nabla_i v_j + \eta J^2 + \nabla \cdot (\kappa_e \nabla T_e) - ac\rho\chi T_e^4 + P_{\mathrm{DT/DD}} + \alpha_{ei}(T_e - T_i);$$

ion specific energy equation:

$$\rho \frac{\partial \epsilon_i}{\partial t} = -\rho \mathbf{v} \cdot \nabla \epsilon_i + [-(P_i+Q) g^{ji} + \sigma^d_{ji}] \nabla_i v_j + \nabla \cdot (\kappa_i \nabla T_i) - ac\rho - \alpha_{ei}(T_e - T_i);$$

magnetic induction:

$$\frac{\partial \mathbf{B}}{\partial t} = -\nabla \times (\mathbf{v} \times \mathbf{B}) - \nabla \times (\eta \nabla \times \mathbf{B}) - \nabla \times \frac{1}{e n_e} (\mathbf{J} \times \mathbf{B});$$

elastic stress:

$$\frac{\partial \sigma^d_{ji}}{\partial t} = 2\mu d_j i^d - v^k \nabla_k \sigma^d_{ji}.$$

An adequate radiation model is also included in this code which calculates the radiation output from different types of plasmas like Kr and DT plasmas.

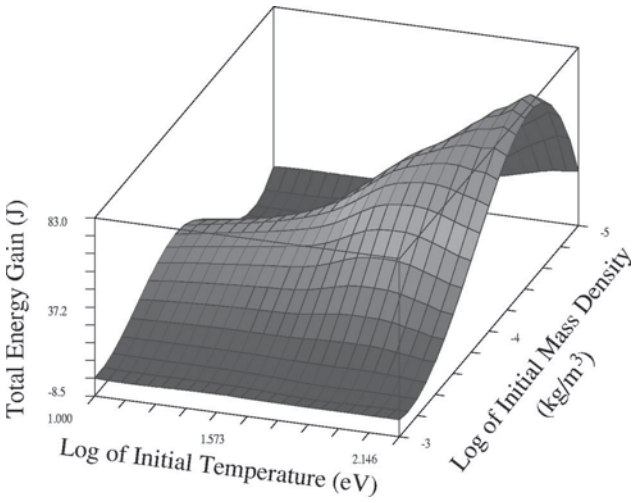

FIG. 2. Fusion energy output as a function of initial mass density and temperature of DT plasma.

III. SIMULATION RESULTS

The main purpose of carrying out the numerical simulation is to investigate the possibility of achieving high yield thermonuclear fusion energy from a low energy Z-pinch machine. We have chosen the parameters of a low energy machine that was designed to test similar types of ideas at the University of California, Irvine. The total inductance of the transmission line of this machine is 25 nH, total capacitance of 50 μf charged to 37.5 kV maximum voltage to date. The current profile produced by the simulation matches well with the experimentally observed profile from a typical shot. Our

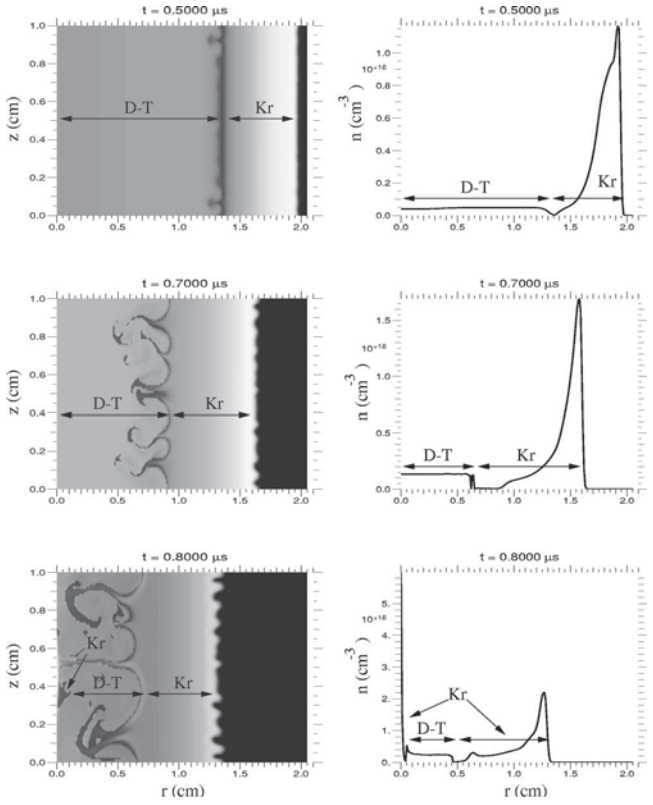

FIG. 4. Density ISO-contours at three different times for $B_z=0$ are shown on the left hand side whereas the right hand side shows the corresponding density profiles at the midplane versus r.

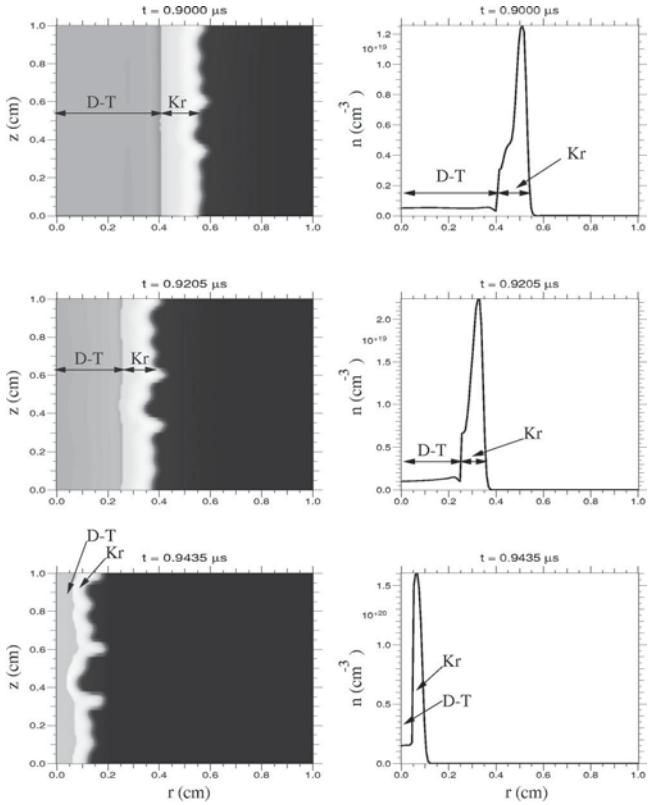

FIG. 5. Density ISO-contours at three different times for $B_z=2$ KG are shown on the left hand side whereas the right hand side shows the corresponding density profiles at the midplane versus r.

first goal is to optimize different controllable parameters in such a manner that the maximum energy of the generator can be transferred to the load at the peak implosion time. Since most of the mass is carried by the outer shell of the Kr plasma, its mass is optimized such that the maximum possible electrical energy transfers to the load in the form of kinetic energy. A 2 kG axial magnetic field is also included because this is a minimum level of axial flux required for the control of RT instability. Once these parameters are fixed, the parameters of the DT core plasma are optimized in order to maximize the neutron yield. For this purpose we used the MACH2 code in the 1-D mode without applying any perturbation. In all these calculations, the injected gas distribution was simulated by a uniform density, right circular cylinder of DT plasma, 1 cm high and 1.9 cm in radius, surrounded by a Kr shell of thickness 0.1 cm. Figure 1 illustrates one of the initial configurations based on UCI Kr–DT gas puff parameters. The electrodes which confine the top and bottom of the load are considered to be perfectly conducting walls. Figure 2 shows the plot of optimized fusion energy output as function of initial density and temperature of the DT plasma. In this figure the vertical z-axis represent the total fusion energy gain (from α particles and neutrons), whereas the x- and y-axes represent the initial temperature and mass of the DT plasma, both these quantities are plotted on a logrithmic scale. There is a sharp peak in the density corresponding to the DT mass density of $1.0\times10^{-7}\,\mathrm{g/cm^3}$ which gives the maximum fusion energy. On the temperature axis the peak is not as sharp as on the density axis. However, some initial heating of the target plasma is necessary for significant energy yield. The peak fusion energy output is around 83 J which corresponds to a neutron yield of 7.0×10^{13}; this is obtained with an initial temperature of 80 eV for the target plasma. The target plasma can be preheated using a plasma gun or by applying an electrical pre-pulse prior to the main implosion pulse.

Figure 3 shows the outer radius of the plasma column $r(t)$, axial plasma density $n(t)$, axial temperature $T(t)$ and neutron yield $Y(t)$ of the target plasma as function of time for the optimum parameter regime. The Kr mass was adjusted to obtain the bang time of ≈0.95 μs to match with experimental bang time at the UCI machine. The stagnation of the plasma column after bang time is due to the fact that peak implosion occurs much before the peak current. Since an initial perturbation is not allowed in a one-dimensional calculation, theoretically the plasma will behave as a confined column up until the current starts decreasing. This figure shows that the density of plasma goes upto $2.5\times10^{19}\,\mathrm{cm^{-3}}$ and the peak temperature reaches up to 14 KeV.

To examine the issue of magnetic shear stabilization of R–T instability in the staged Z pinch, a number of 2-D MHD calculations are performed using this code. The optimum parameter of Kr plasma and DT plasma obtained from 1-D calculations are used. In these calculations, a configuration similar to Fig. 1 is used together with an initial perturbation of density. Initially a random cell-to-cell density throughout the cylinder was introduced into the calculation. The cell

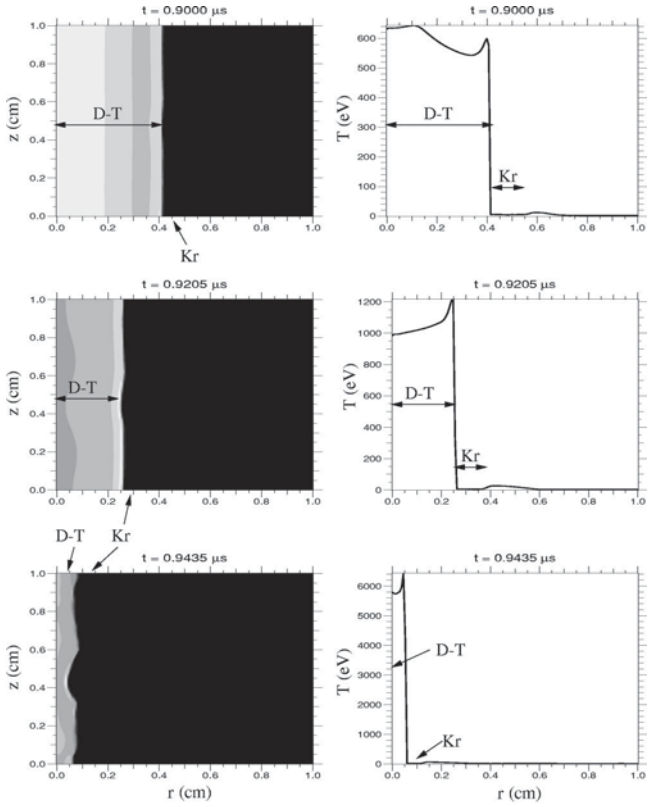

FIG. 6. Temperature ISO-contours at three different times for $B_z = 2$ KG are shown on the left hand side whereas the right hand side shows the corresponding density profiles at the midplane versus r.

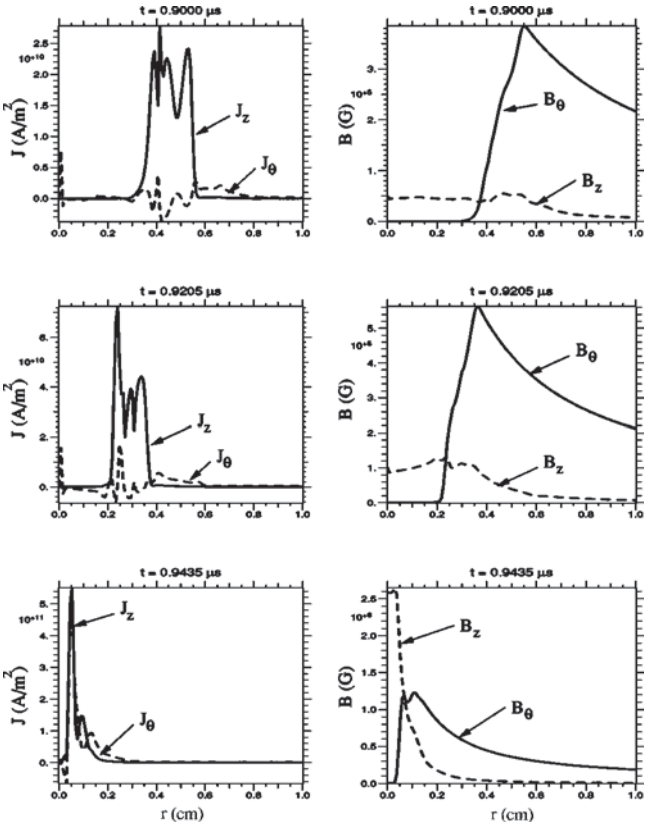

FIG. 7. For $B_z = 2$ KG the profiles of axial and azimuthal current density profiles at the midplane versus r are shown on the left hand side whereas the magnetic field profiles are on the right hand side.

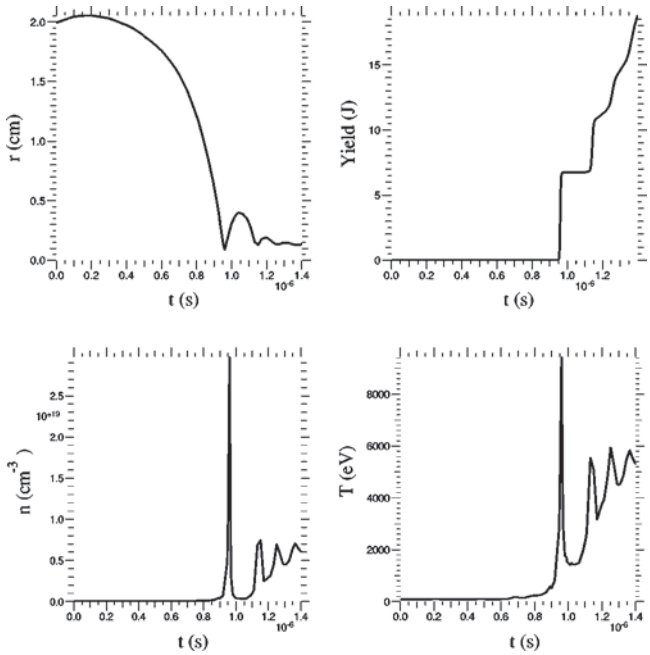

FIG. 8. Plots of pinch radius $r(t)$, axial plasma density $n(t)$, axial plasma temperature $T(t)$ and fusion yield $Y(t)$ versus time obtained from a 1-D simulation run for $B_z = 4$ KG.

resolution along the pinch axis is 0.01 cm, allowing wavelengths as small as 0.5 mm. To follow the evolution of the RT-instability, the calculations were run in a Eulerian mode and were carried out both with and without the axial magnetic field. Without any axial magnetic field the pinched plasma becomes highly unstable due to the rapid growth of RT instability during the early stages of implosion. Finally the simulation gets terminated at about 0.8 μs. By applying a 2 kG axial magnetic field the growth of RT instability is significantly reduced and the simulation can run up to 0.9435 μs. The simulation results of the early phase of implosion for the case of no axial magnetic field is shown in Fig. 4, which describes the density ISO-contours for three different time steps up until 0.8 μs. It is clear from Fig. 4 that in the case of no axial magnetic field the pinch becomes highly unstable in the very early stages of the implosion. The instability predominantly appears in the inner region of the DT plasma, whereas the growth of instability in the Kr shell is slower. Ultimately the entire shell becomes highly unstable and the calculation terminates almost 200 ns before the peak implosion. The neutron yield up to this point is insignificant. Observing the current and magnetic field profiles we can explain this behavior. The axial current easily diffuses through the outer plasma shell and transfers to the inner boundary of the DT plasma. The rapid diffusion through the Kr plasma is due to the higher resistivity caused by radiative cooling. Because of the much lower resistivity of the inner DT plasma resulting from its poor radiative efficiency, diffusion of magnetic field and current through the inner plasma region is rather difficult. Since the DT plasma column is much lighter in mass than the outer Kr plasma shell, it implodes at a much faster rate. This increased level of acceleration causes the instability to grow in the inner region faster than in the outer

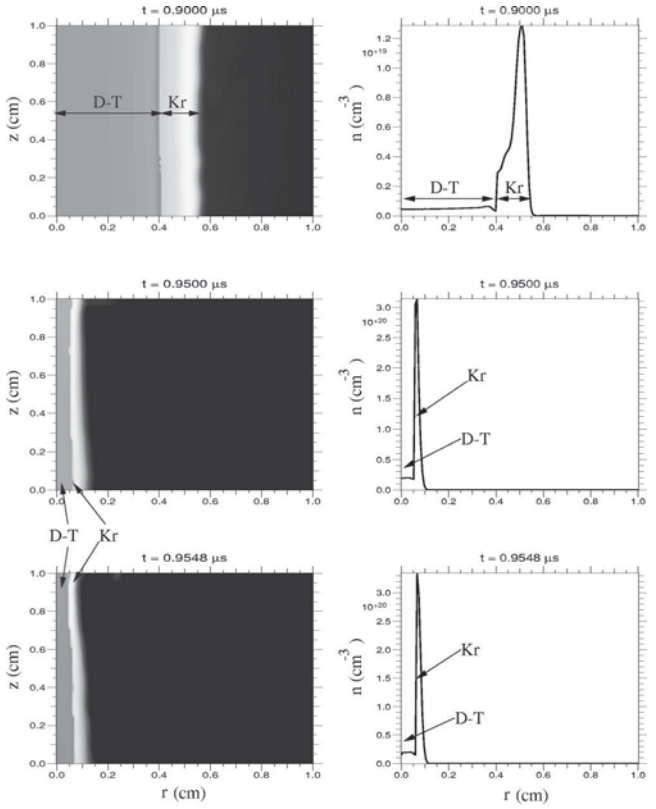

FIG. 9. Density ISO-contours at three different times for $B_z=4$ KG before the peak compression are shown on the left hand side whereas the right hand side shows the corresponding density profiles at the midplane versus r.

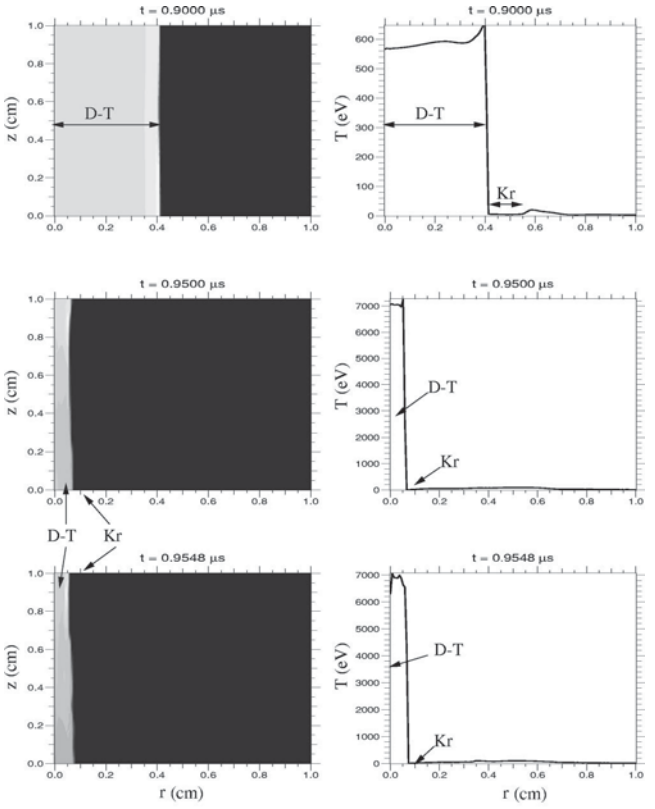

FIG. 10. Temperature ISO-contours at three different times for $B_z=4$ KG before the peak compression are shown on the left hand side whereas the right hand side shows the corresponding density profiles at the midplane versus r.

shell region. Figure 5 also shows that the inclusion of an axial magnetic field improves the stability significantly. Particularly the inner plasma column remains stable up until the peak implosion. However, the outer boundary of the outer shell becomes unstable but with a significantly reduced growth rate. The case with 2 KG of axial magnetic field ran up to 0.9435 μs and the results of the later stage of implosion are presented in Figs. 5, 6 and 7. The density ISO-contours at three different times of implosion are shown in Fig. 5 and temperature ISO-contours are shown in Fig. 6. The plots on the left hand sides are shown for a typical r-z plane, whereas the ones on the right hand side are profiles of density and temperature at the midplane versus r. In each calculation the total mass of Kr is 3.5×10^{-4} g/cm^3 and DT-mass is 1.0×10^{-7} g/cm^3 which is insignificant as compared to the Kr mass. The peak current delivered to the load was typically 1 MA, with implosion times (or quarter period rise time of the current) of 1 μs which compares with the experimental profile. During the implosion, Kr plasma remains significantly cooler than the DT plasma due to the enhanced radiation loss of thermal energy. As a consequence, the density of the Kr plasma becomes much higher as the compression progresses. Interestingly no mixing is observed between the two plasmas during the entire phase of implosion, although it was allowed in the simulation model. The reason for this is obvious from Fig. 7, which shows the current and magnetic field profiles at the midplane of the z-axis. There is a strong compression of the magnetic field in between the two plasmas which isolates both plasmas from each other. Just for comparison the one-dimensional results for the case of $B_z=4$ KG are presented in Fig. 8. Again the profiles of outer radius $r(t)$, axial plasma density $n(t)$, axial plasma temperature $T(t)$ and fusion yield $Y(t)$ are plotted as a function of time. Some reduction in fusion yield, peak plasma density and temperature is due to the fact that the pinch is softer because of the increased level of trapped axial magnetic flux.

Figures 9–14 represent the implosion with the same parameters as of Figs. 5–7 but the axial magnetic field is increased to 4 KG instead of 2 KG. The left hand side of Figs. 9 and 12 represent two sets of density ISO-contours at six different times: two before the implosion and four after the implosion. The peak implosion time is at 0.95 μs describing a minimum radius of the pinched column. Up until the peak implosion time no significant distortion is observed. A small level of surface perturbation is apparent at the inner and outer surface of the Kr plasma shell that may be due to an extremely slow growth rate of RT-instability. Figure 12 presents three snapshots of density ISO-contours after the peak implosion time and up until 1.0 μs. This figure clearly shows the growth of an instability that is similar to the sausage mode ($m=0$) but with an asymmetric growth along the z-axis. This is due to a strong axial flow of plasma which emerges after the peak implosion time. Axial plasma flow develops due to $\mathbf{J}\times\mathbf{B}$ force when $\mathbf{J}$ acquires a radial component due to an uneven growth of the sausage instability. Both

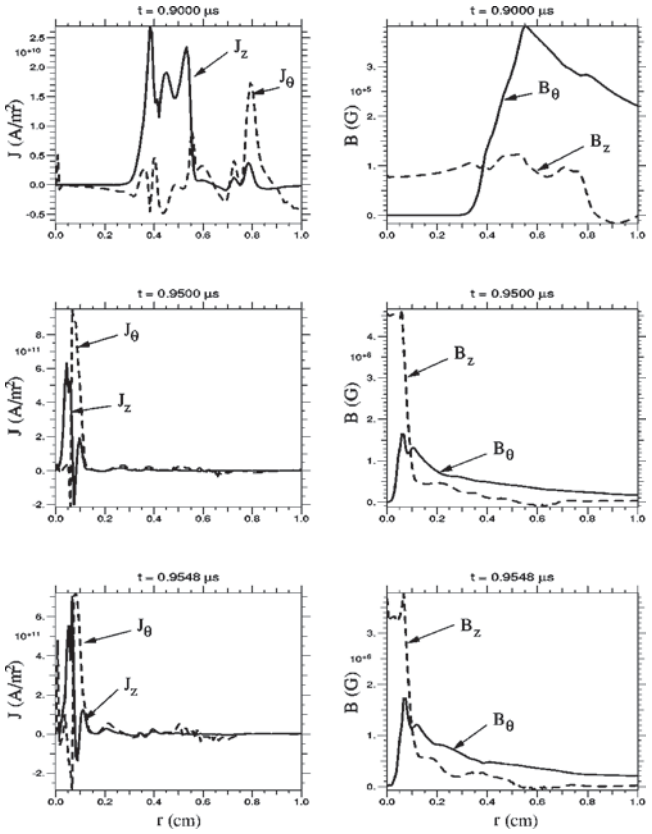

FIG. 11. Before the peak compression and for $B_z = 4$ KG the profiles of axial and azimuthal current density profiles at the midplane versus r are shown on the left hand side whereas the magnetic field profiles are on the right hand side.

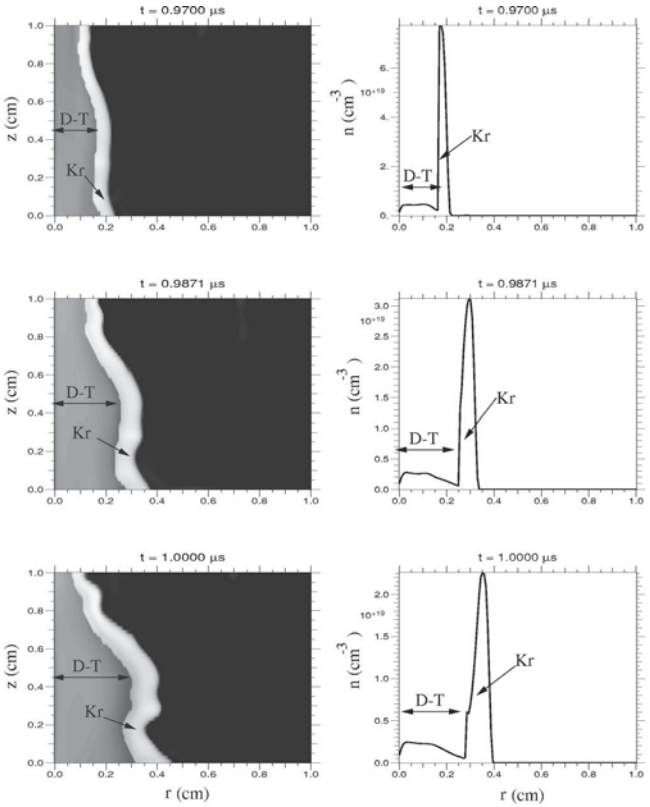

FIG. 12. Density ISO-contours at three different times for $B_z = 4$ KG after the peak compression are shown on the left hand side whereas the right hand side shows the corresponding density profiles at the midplane versus r.

Kr and DT plasmas remain isolated even during the growth of this instability. The left hand sides of Figs. 10 and 13 are corresponding temperature ISO-contours which show the perfect stability and uniformity of the DT-plasma column up until the peak implosion time. The right hand sides of all these figures are profiles of density and temperature at the midplane versus r. The highest value of the temperature of DT plasma is about 7 keV whereas for 2 kG it is less than 6 keV. Without any axial magnetic field the temperature never achieved more than few hundred electron-volts. This clearly demonstrates an enhanced level of energy coupling to the DT load by controlling the growth of the RT-instability. Figures 11 and 14 show the current density and magnetic field profiles versus r at the midplane. From Fig. 11 it is apparent that at the outer boundary of the Kr plasma shell the values of both B_z and B_θ is approximately 1.0 MG; this produces a strong magnetic shear which stabilizes the RT-type instabilities. Compare it with Fig. 7 where the value of B_θ was also 1.0 MG but the value of B_z is between 100 to 300 KG. This represents a weak shear in the total magnetic field limiting the growth of RT-instability but not completely eliminating it. During the implosion some axial current diffuses through the Kr plasma shell and starts flowing on the surface of the DT plasma column. This diffused current gets amplified at the peak implosion to a value comparable to the outer current. In Fig. 11 it is also apparent that oppositely directed azimuthal currents are flowing on the inner surface of the Kr

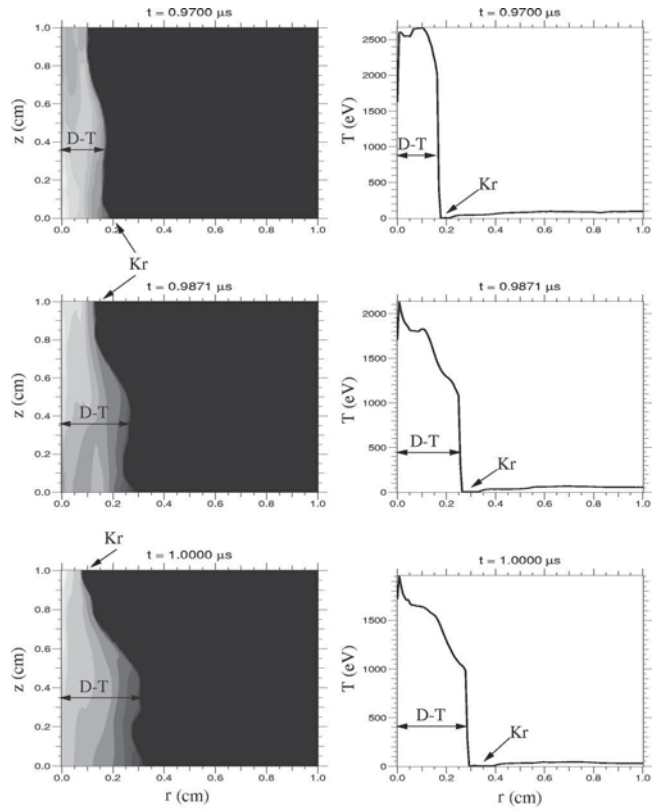

FIG. 13. Temperature ISO-contours at three different times for $B_z = 4$ KG after the peak compression are shown on the left hand side whereas the right hand side shows the corresponding density profiles at the midplane versus r.

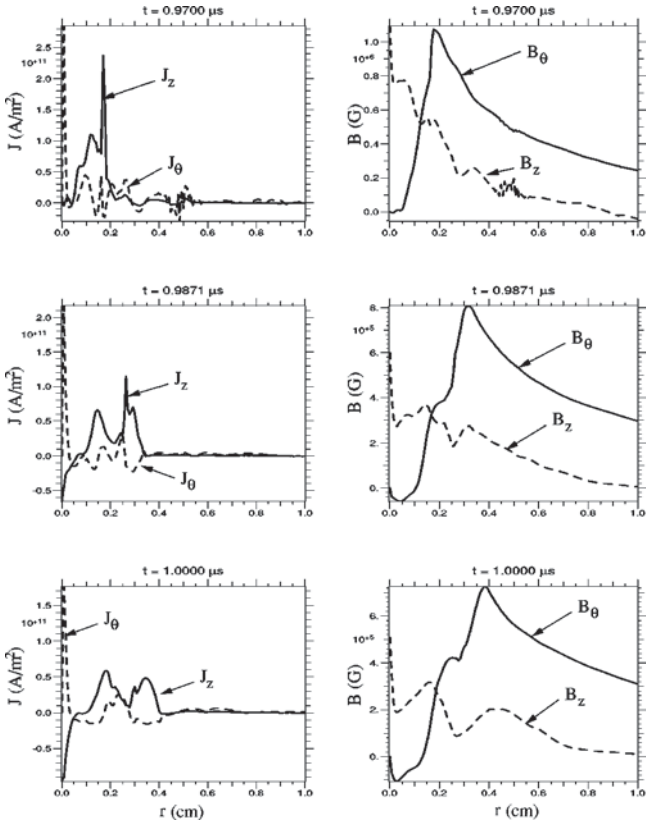

FIG. 14. After the peak compression and for $B_z = 4$ KG the profiles of axial and azimuthal current density profiles at the midplane versus r are shown on the left hand side whereas the magnetic field profiles are on the right hand side.

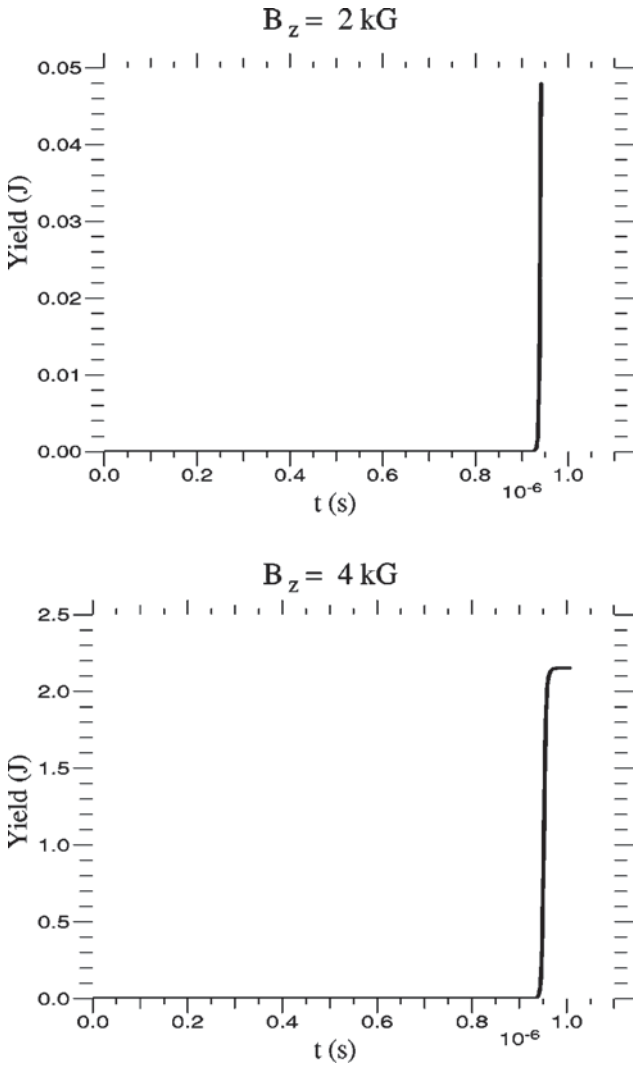

FIG. 15. Fusion yield as a function of time obtained from a 2-D simulation run for $B_z = 2$ KG and $B_z = 4$ KG.

plasma shell and the outer surface of the DT plasma column. This develops due to the large value of $\partial B/\partial t$. The azimuthal current seems to exceed the axial current at the time of peak implosion. This may be due to the compression of the pinched plasma beyond equilibrium as a result of inertia. This type of current amplification from flux compression has been predicted in the past by Rahman *et al.*[5,15] The fusion yields for both cases with $B_z = 2$ KG and $B_z = 4$ KG as a function of time are presented in Fig. 15 which shows that for $B_z = 2$ KG is almost two orders of magnitude smaller than for $B_z = 4$ KG when the RT-instability was completely eliminated. This shows that elimination of instability dramatically enhances the energy coupling to the load.

IV. CONCLUSION

The research on controlled fusion energy over the past few decades has led to the construction of big machines capable of holding multi-megajoules of energy. To achieve break-even and beyond, the popular concepts may require even larger energies than the existing machines. The complexity and cost of these machines may impede the construction of future machines, leading to a halt in testing ideas related to controlled thermonuclear fusion. On the other hand, the *Z* pinch is the simplest and the cheapest of all types of fusion machines. The MJ class of *Z*-pinch machines may not be attractive for any kind of energy production because the entire load region needs to be replaced after each shot. However they may be useful for testing concepts and other defense related applications. The 50 KJ to few 100 kJ machines can be operated on a high repetition rate without breaking the vacuum. Such low to medium energy machines are ideally most suitable for controlled thermonuclear fusion related experiments.

In this paper we have discussed the possibility of achieving high yield controlled thermonuclear energy from a 50 kJ machine using the innovative concept of staging the implosion and thus controlling the instabilities. We considered the simplest configuration that can be easily implemented on the several types of existing 50–100 kJ class machines. It is shown that the most dangerous instabilities, like RT type instabilities, can be controlled. The control of these instabilities leads to an efficient energy coupling. Besides controlling the instabilities, the rapid transfer of energy to the target plasma is also crucial in order to avoid radiative losses in the target plasma. Staging permits the use of long pulse machines since at each stage the duration of energy transfer becomes shorter by many orders of magnitude.

Optimization of different parameters seems to be very

important for achieving highest thermonuclear yield. We have only optimized the parameters of the target plasma keeping the machine parameters fixed. In reality all parameters need to be optimized including the machine parameters, type and shape of the liner, etc., and in this way one may find a regime that could lead to the net production of fusion energy from a small size machine. Future studies will focus on the optimization of the remaining parameters.

ACKNOWLEDGMENTS

We thank R. E. Peterkin, J. H. Degnen and Phillips Laboratory for providing the MACH2 code. This work has been supported by Office of Fusion Energy, Department of Energy.

[1]M. K. Matzen, Phys. Plasmas **4**, 1519 (1997).
[2]R. B. Spielman, R. J. Dukart, D. L. Hanson, B. A. Hammel, W. W. Hsing, M. K. Matzen, and J. L. Porter, in *Proceedings of the 2nd International Conference on Dense Z Pinches*, Laguna Beach, CA, 1989, edited by N. R. Pereira, J. Davis, and N. Rostoker (American Institute of Physics, Melville, New York, 1989), p. 3.
[3]C. Deeney, M. R. Douglas, R. B. Spielman, T. J. Nash, D. L. Peterson, P. L'Eplattenier, G. A. Chandler, J. F. Seamen, and K. W. Struve, Phys. Rev. Lett. **81**, 4883 (1998).
[4]M. R. Douglas, C. Deeney, and N. F. Roderick, Phys. Rev. Lett. **78**, 4577 (1997).
[5]A. L. Velikovich and S. M. Golberg, Phys. Fluids B **5**, 1164 (1993).
[6]F. L. Cochran, J. Davis, and A. L. Velikovich, Phys. Plasmas **2**, 2765 (1995).
[7]R. B. Baksht, I. M. Datsko, A. A. Kim *et al.*, Fiz. Plazmy **21**, 959 (1995) [Plasma Phys. Rep. **21**, 907 (1995)].
[8]V. Smirnov, Plasma Phys. Controlled Fusion **33**, 1697 (1991).
[9]T-F. Chang, A. Fisher, and A. Van Drie, J. Appl. Phys. **69**, 3447 (1991).
[10]S. Chandrasekar, *Hydrodynamic and Hydromagnetic Instability* (Dover, New York, 1981).
[11]S. A. Sorokin, A. V. Khachaturyan, and S. A. Chaikovskii, Sov. J. Plasma Phys. **17**, 841 (1991).
[12]A. B. Bud'ko, M. A. Liberman, L. Velikovich, and F. S. Felber, Phys. Fluids B **2**, 1159 (1990).
[13]H. U. Rahman, F. J. Wessel, and N. Rostoker, Phys. Rev. Lett. **74**, 714 (1995).
[14]H. U. Rahman, P. Ney, F. J. Wessel, and N. Rostoker, J. Plasma Phys. **58**, 367 (1997).
[15]H. U. Rahman, P. Ney, F. J. Wessel, A. Fisher, and N. Rostoker, *High Density Pinches*, 2nd International Conference, Laguna Beach, 1989 (American Institute of Physics, Melville, New York), p. 195.
[16]A. Chuvatin, P. Choi, and B. Etlicher, Phys. Rev. Lett. **76**, 2282 (1996).
[17]J. H. Degnan, R. E. Peterkin, Jr., G. P. Baca *et al.*, Phys. Fluids B **5**, 2938 (1993).
[18]R. E. Peterkin, Jr. *et al.*, IEEE Trans. Plasma Sci. **21**, 552 (1993).